Available online at www.sciencedirect.com

ScienceDirect

Ceramics International 40 (2014) 3411–3418

CERAMICS INTERNATIONAL

www.elsevier.com/locate/ceramint

# Effects of BN/SiC dual-layer interphase on mechanical and dielectric properties of $SiC_f$/SiC composites

Yang Mu*, Wancheng Zhou, Fa Luo, Dongmei Zhu

*State Key Laboratory of Solidification Processing, Northwestern Polytechnical University, Xi'an, Shaanxi 710072, China*

Received 17 August 2013; received in revised form 16 September 2013; accepted 20 September 2013
Available online 26 September 2013

**Abstract**

BN/SiC dual-layer interphase in $SiC_f$/SiC composites was successfully prepared using urea–boric acid solution as precursor for dip-coating process and PCS/xylene solution for PIP process. XRD and Raman spectrum results show that both BN and SiC sub-layers have relatively low crystalline degree. The surface of as-prepared BN/SiC dual-layer interphase is smooth and homogeneous, and its thickness is about 0.42 μm. The flexural strength and failure displacement of composites with BN/SiC dual-layer interphase are improved conspicuously to 272 MPa and 0.26 mm, which are both much higher than those of composites without interphase, whose ultimate values are only 126 MPa and 0.14 mm, respectively. The composites with dual-layer interphase show better anti-oxidation capability than do the composites with BN interphase below 1000 °C. $\varepsilon'$ and $\varepsilon''$ of the composites increase from $30-i22$ to $45-i32$ after incorporation of dual-layer interphase, which are caused by relaxation polarization and conductance losses established in the components, including fibers, matrix and interphase.


*Keywords:* B. Composites; C. Dielectric properties; C. Mechanical properties; BN/SiC dual-layer interphase

## 1. Introduction

$SiC_f$/SiC composites have been developed as promising structural or functional materials for applications in advanced aerojet engines, stationary gas turbines and nuclear fusion reactors due to their excellent properties, such as high strength, high thermostability, low density, high resistance to corrosion and microstructural stability under neutron irradiation [1]. The main advantages of $SiC_f$/SiC composites with respect to their monolithic counterparts lie in the fact that they can be converted into toughened materials by introducing a proper design of fiber/matrix interphase to impede microcracks formed under load in the matrix and to prevent early failure of the fibrous reinforcement, although their constituents are intrinsically brittle [2]. It has been recognized that the best interphases might be those with a laminar structure, such as PyC [3–5] and h-BN [6–8], or a multi-layered microstructure, such as $(PyC–SiC)_n$ [9,10] and $(BN–SiC)_n$ [11,12] (say, $(X–Y)_n$), the layers being coated alternately and parallel to the fiber surface. Compared with the single-layered interphase, the multi-layered interphase can be widely tailored, such as the elemental types of $X$ and $Y$, the sequence number $n$ and the thickness of $X$ and $Y$ sub-layers. What is more, the functions of interphase can be decoupled with the result that the layer $X$ can act as a mechanical fuse to maintain good load transfer and the layer $Y$ can act as diffusion barrier during the composites processing [13].

From the mechanical standpoint, the optimized interphase synthesized in $SiC_f$/SiC composites provides improvements not only in toughening the composites, but also in extending lifetime under oxidizing atmosphere at elevated temperatures. In comparison with BN, PyC is oxidation prone even at low temperatures, whose oxidizing temperature is about 450 °C versus 800 °C for BN [14]. Hence, the PyC interphase becomes the weak point for $SiC_f$/SiC composites when used in oxidizing atmosphere. On the other hand, the PyC interphase is not appropriate for microwave absorbing applications of $SiC_f$/SiC composites because it can lead to strong reflection of electromagnetic wave due to its high electrical conductivity [15]. Consequently, BN with low electrical conductivity is one of the ideal interphase materials for microwave

*Corresponding author. Tel./fax: +86 29 88494574.
*E-mail addresses:* muyang300847@gmail.com, 753340357@qq.com (Y. Mu).

0272-8842/$ - see front matter © 2013 Elsevier Ltd and Techna Group S.r.l. All rights reserved.
http://dx.doi.org/10.1016/j.ceramint.2013.09.091

absorbing applications of $SiC_f/SiC$ composites [16]. In addition, SiC has been extensively investigated for microwave absorbing applications by many researchers in recent years. H. Tian et al. [17] synthesized a kind of C-enriched α-SiC powders through combustion process and reported its effects on dielectric properties of $SiO_{2f}/SiO_2$ composites in the frequency range of 8–18 GHz. This revealed that the SiC powders enhanced the complex permittivity of the composites and a bandwidth of 5 GHz with the reflectivity below −10 dB was obtained for the composites with 20 wt% SiC powders. H. T. Liu et al. [18] studied the effects of high temperatures on dielectric properties of $SiC_f/SiC$ composites prepared by PIP process. The results indicated that both the real and imaginary parts of complex permittivity increased with increasing temperatures. Q. Li et al. [19] prepared porous SiC ceramics using polycarbosilane as precursor by PIP process and investigated the effects of annealing temperatures on microwave absorption properties of the ceramics in X band. As reported, an excellent microwave absorption property with average reflectivity of −9.9 dB was achieved for the sample annealed at 1400 °C. In this work, SiC will be prepared as interphase materials for functional and mechanical purpose.

Various processes have been developed for the preparation of BN and SiC interphases [20–23]. By comparison, dip-coating for BN interphase and PIP process for SiC interphase are the proper methods for preparation of BN/SiC dual-layer interphase, which display several important advantages: (1) simple organic or inorganic precursors are available for the interphase materials of interest; (2) they are low-temperature and low-pressure processes with no significant degradation of the fibers. Up to now, much attention has been mainly focused on the preparation and characterization of BN/SiC dual-layer interphase [11,24], while the reports on mechanical and dielectric properties of $SiC_f/SiC$ composites with BN/SiC dual-layer interphase are rare.

In the present work, the microstructure of prepared BN and SiC sub-layers was characterized, and the effects of BN/SiC dual-layer interphase on mechanical properties, oxidation resistance and dielectric properties of $SiC_f/SiC$ composites were investigated.

## 2. Experimental procedure

### 2.1. Preparation of the interphase and composites

The KD-I SiC fiber bundles used as the reinforcement were provided by National University of Defense Technology, China. General characteristics of the fibers were described elsewhere [22]. The 2.5D shallow straight-joint fabrics were braided by Nanjing Glass Fiber Institute, China, and the fiber volume fraction was 40%. PCS powders with molecular weight ~1800 and softening point ~180 °C were provided by National University of Defense Technology, China.

Prior to interphase preparation, the SiC fabrics were desized in vacuum at 700 °C for 1 h and ultrasonically cleaned in acetone solution for 15 min. The BN sub-layer was synthesized on the fiber surface, and then the SiC sub-layer. Preparation route of $SiC_f/SiC$ composites with BN/SiC dual-layer interphase is shown in Fig. 1. For preparation of BN sub-layer, 0.05 mol boron acid and 0.60 mol urea were mixed together and dissolved in the mixture of 100 ml deionized water and 200 ml ethanol. The mixture was ultrasonically stirred for 10 min in order to mix and dissolve sufficiently. The multiple fabrics were dipped into the urea–boric acid solution for 10 min in vacuum. After infiltration, these fabrics were dried at 50 °C using an electric air blowing dryer. Finally, the samples were heated at a rate of 5 °C/min in nitrogen to 1000 °C for 2 h in a vacuum sintering furnace (ZRS-150, San Te, Jinzhou, China). The SiC sub-layer was derived from PCS/xylene solution with a concentration of 10 wt%. The SiC fabrics with BN sub-layer were dipped into the PCS solution in vacuum for 15 min. After infiltration and drying, the samples were heated to 1100 °C and held for 2 h.

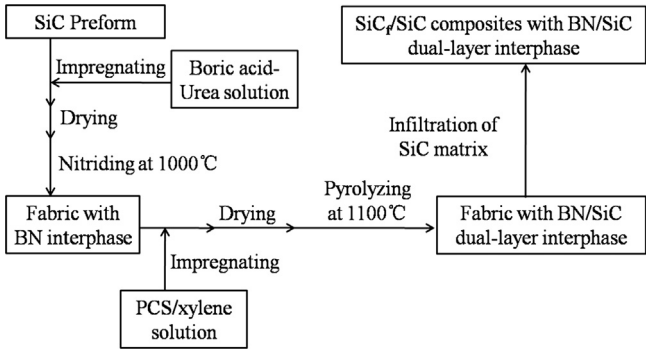


Fig. 1. Preparation route of $SiC_f/SiC$ composites with BN/SiC dual-layer interphase.

The SiC fabrics were densified with SiC matrix using the thermal decomposition of methyltrichlorosilane (MTS). $H_2$ was chosen as carrier gas and diluent gas with flow ratios of 30 and 300 ml/min, respectively. The CVD densification process was carried out at 1000 °C for 16 h for each composite at 8 kPa in the reactor.

### 2.2. Characterization

The microstructure of prepared interphases was characterized by X-ray diffraction (X'Pert PRO MPD, PANalytical, Almelo, The Netherlands) and Raman spectroscopy (LabRAM HR800). The surface morphologies of prepared interphases and as-received fracture surface of composites after three-point bending tests were characterized by a scanning electron microscope (Model SUPRA-55, Zeiss, Germany).

The open porosity of the samples was tested by the Archimedes method. Three-point bending test (specimen size of $40^l$ mm × $4^w$ mm × $3^t$ mm) was carried out at ambient temperature with a cross-head speed of 0.5 mm/min and support span length of 30 mm using a universal testing machine (Haida Qualitative Analysis, HD-609B). Specimens were cut parallel to the longitudinal direction, and the test was conducted following the general guidelines of ASTM standard C 1341, using five specimens. $\sigma$ was calculated by the following equation:

$$\sigma = 3FL/2bh^2 \quad (1)$$

where $F$ is the load at a point of deflection of a load–displacement curve in test, $L$ is the support span length, $b$ is the specimen width, and $h$ is the specimen thickness.

The real part ($\varepsilon'$) and imaginary part ($\varepsilon''$) of complex permittivity that correlate polarization and dielectric loss were measured in the frequency range of 8.2–12.4 GHz by the waveguide method using a vector network analyzer (E8362B). The dimensions of measured samples were 22.86 mm × 10.16 mm × 2.0 mm.

## 3. Results and discussion

### 3.1. Microstructure and morphology of prepared interphases

Fig. 2 shows the XRD pattern and Raman spectrum of prepared BN interphase. It is found in Fig. 2(a) that an obvious peak around $2\theta$ value of 26.5° is detected, which corresponds to (002) crystal plane of t-BN [20]. And other diffractions at 42° (100), 55° (004), and 76° (110) are also discernible. The Raman spectrum in Fig. 2(b) displays that only one broad peak located at near 1380 $cm^{-1}$ is observed, which is the $E_{2g}$ band that resulted from the vibration of B–N bond, corresponding to the characteristic of t-BN [25]. These results show that the dip-coated BN interphase has relatively low crystalline degree. Surface morphologies of original and BN coated SiC fibers are shown, respectively, in Fig. 3(a) and (b). In Fig. 3(a), the surface of original SiC fibers is inhomogeneous and contains some defects. After dip-coating, shown in Fig. 3(b), the fibers are carpeted with smooth and uniform BN interphase, and part of interphase spalling on fiber surface can be observed. It is detected in Fig. 3(c) that the thickness of BN sub-layer is about 0.2 μm.

Fig. 4 shows the XRD pattern and Raman spectrum of prepared SiC interphase. In the XRD pattern shown in Fig. 4 (a), three obvious peaks around $2\theta$ values of 35.7°, 60.4° and 71.8° correspond to (111), (220) and (311) reflections of β-SiC, respectively. The broad bands show that the crystalline degree of β-SiC is not complete. The Raman spectrum in Fig. 4 (b) shows that two relative broad bands at about 1380 and 1580 $cm^{-1}$ are detected, which are called D and G bands of carbon respectively. The D and G peaks indicate that the PIP-SiC interphase has carbon excess [26]. The SiC peaks cannot be detected because the Raman scattering efficiency of carbon species can be assumed to be at least ten times higher than that of pure SiC due to their optical absorption [27]. The above results exhibit that the interphase is an amorphous state embedded with β-SiC and carbon micro-crystals. The surface and cross-section SEM images of SiC fibers with SiC interphase are shown in Fig. 3(d) and (e). It appears in Fig. 3(d) that the interphase formed at 1100 °C is continuous and uniform, except that a few delaminations exist on the surface. The thickness of SiC sub-layer is about 0.2 μm, shown in Fig. 3(e).

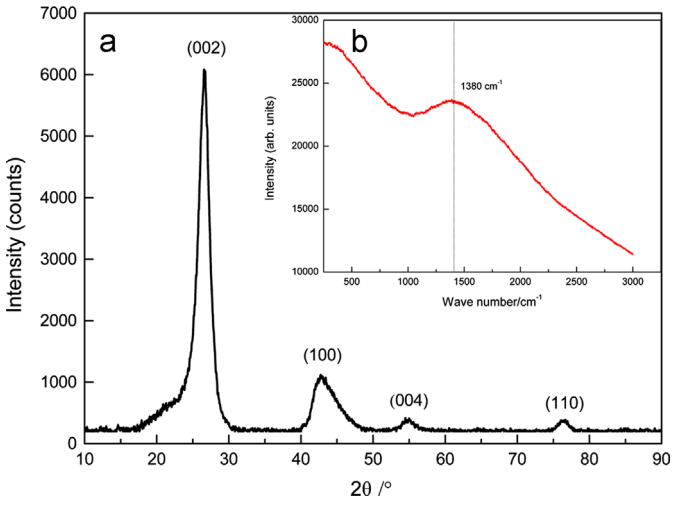


Fig. 2. (a) XRD pattern and (b) Raman spectrum of prepared BN interphase.

Fig. 5 shows the surface morphologies of SiC fibers with BN/SiC dual-layer interphase. After dip-coating and PIP process, the fibers are covered obviously by interphase and their surfaces are relatively smooth except for molten state delamination on some filaments, shown in Fig. 5(a) and (b). The thickness of as-prepared dual-layer interphase is estimated to be about 0.42 μm shown in Fig. 5(c). Although there are some defects on the fiber surface, hardly any representative fiber bridging can be seen in Fig. 5(d). In $SiC_f$/SiC composites, a proper surface morphology of the interphase is necessary for the purpose of minimizing stress concentration and having the correct crack deflection behavior [28].

### 3.2. Mechanical properties of $SiC_f$/SiC composites with BN/SiC dual-layer interphase

#### 3.2.1. Effects of dual-layer interphase on mechanical properties

Properties of the fabricated $SiC_f$/SiC composites without and with BN/SiC dual-layer interphase are listed in Table 1. The flexural strength and failure displacement of composites with interphase are 272 MPa and 0.26 mm respectively, which are both much higher than those of composites without interphase, whose ultimate values are at only 126 MPa and 0.14 mm, even though no obvious differences in bulk density and porosity are observed. It can be seen that the flexural strength and failure displacement of $SiC_f$/SiC composites are significantly improved two times after preparation of BN/SiC dual-layer interphase.

Fig. 6 shows the typical stress–displacement curves of $SiC_f$/SiC composites fabricated without and with interphase. It is observed in Fig. 6 that sample (a) without interphase shows low flexural strength and fails in a catastrophic manner. With the incorporation of BN/SiC dual-layer interphase, the fracture behavior is completely changed and the curve of the composites exhibits standard toughened fracture behavior, as displayed in sample (b). When the load reaches maximum, the curvilinear trend will decline gradually, and then considerably increased failure displacement is observed for composites with interphase. The much larger extended area under the curve of sample (b) indicates that much larger amount of fracture energy is consumed during the composites fracture [9]. This can be further supported by the fracture surface morphologies of $SiC_f$/SiC composites shown in Fig. 7. As seen from Fig. 7(a), the composites without interphase show hardly any

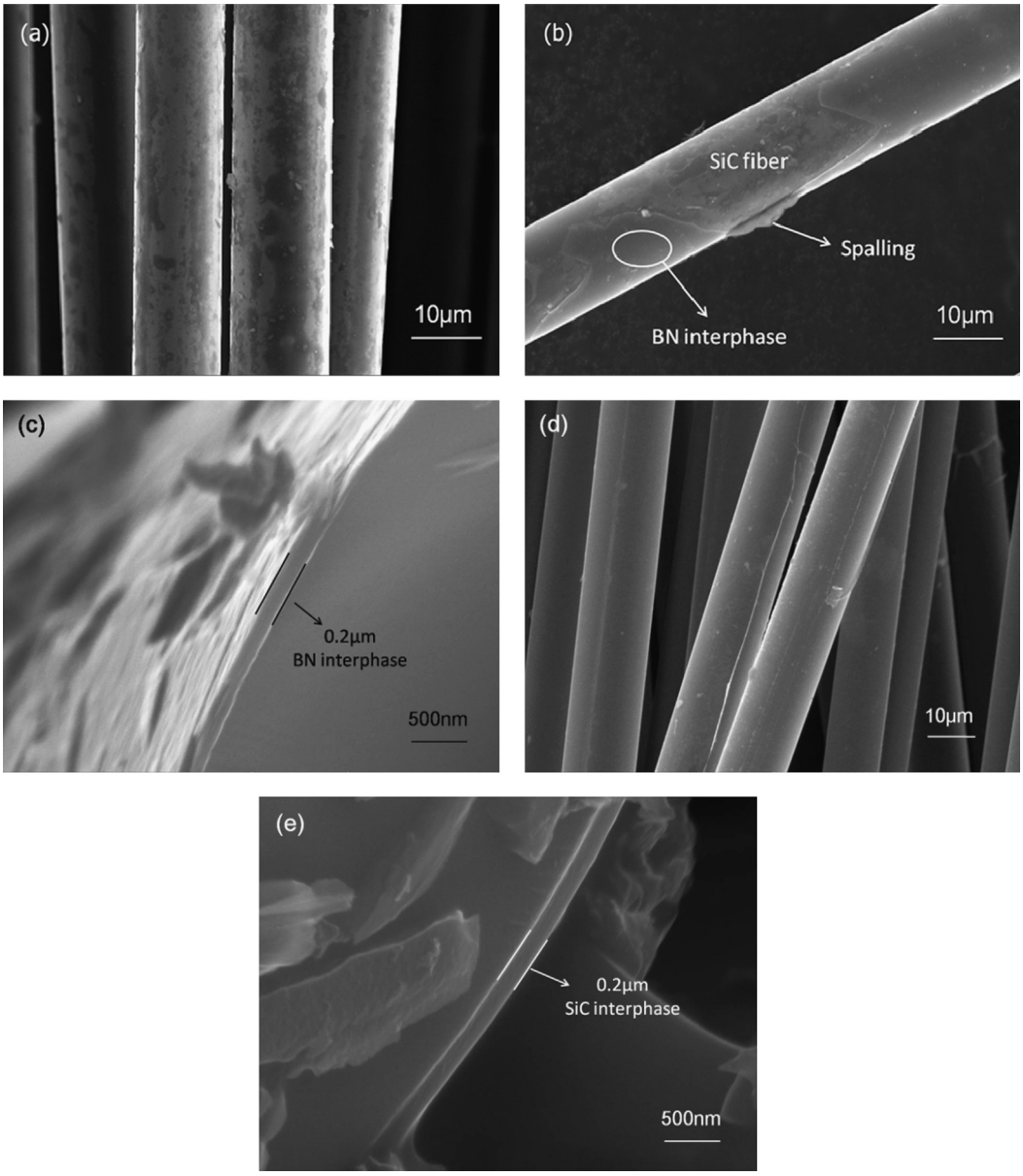


Fig. 3. Surface morphologies of the SiC fibers: (a) as received; (b, c) with BN interphase; and (d, e) with PIP-SiC interphase.

fiber pull-out. In the case of composites with interphase shown in Fig. 7(b), extensive fibers debonding and pull-out are observed in the fracture surface, and the surface of pull-out fibers is smooth and free of any matrix.

Generally, the mechanical properties of $SiC_f$/SiC composites are determined by the interfacial bonding strength and in situ fiber strength [29]. During the CVI process, plenty of aggressive gas will be generated from the decomposition of intermediate silicon and carbon species. The SiC fabrics are seriously damaged by the aggressive gas when there is no interphase. According to Ref. [30], a turbostratic PyC interphase around 30 nm is found on the surface of KD-I SiC fibers. Although the slight interphase is favorable for the mechanical property improvement of $SiC_f$/SiC composites by PIP process, it is difficult to form an effective barrier layer to prevent elemental interdiffusion and chemical reactions during such a long period of CVI process, since the fracture surface is even and hardly any fiber debonding can be observed in Fig. 7 (a). Simultaneously, defects existing on the surface of original SiC fibers would lead to strong physical interfacial bonding with SiC matrix. Thus, the low fiber strength and strong interfacial bonding would make the reinforcing mechanisms invalid and a brittle fracture behavior occurs in the as-received $SiC_f$/SiC composites.

As it is well known that BN and PIP-SiC are both inert materials, it can play a diffusion barrier part at the interface to protect the fibers from chemical damage when introducing the BN/SiC dual-layer interphase. Obvious fiber/interphase interfacial debonding phenomena are detected in Fig. 7(c), indicating that the dual-layer interphase effectively weakens the chemical

interfacial bonding to the fibers. Moreover, the interphase helps to compensate for the defects on SiC fibers to reduce the stress concentration. Based on the results in previous study [22], the PIP-SiC interphase weakens the fiber/matrix interfacial bonding and an obvious debonding is observed in the fiber/interphase interface, which indicates that no elemental diffusion occurs and a weak bonding forms between the PyC surface layers and PIP-SiC interphase. Similarly, when the cracks propagate from matrix to the fibers, possible crack deflection and interfacial debonding also can take place between the turbostratic BN layer and PIP-SiC layer, though no obvious debonding behavior is observed in these interfaces. From the analysis above, it indicates that the BN/SiC dual-layer interphase significantly decreases the fibers damage and provides appropriate interfacial bonding for $SiC_f$/SiC composites, which results in adequate fracture toughness.

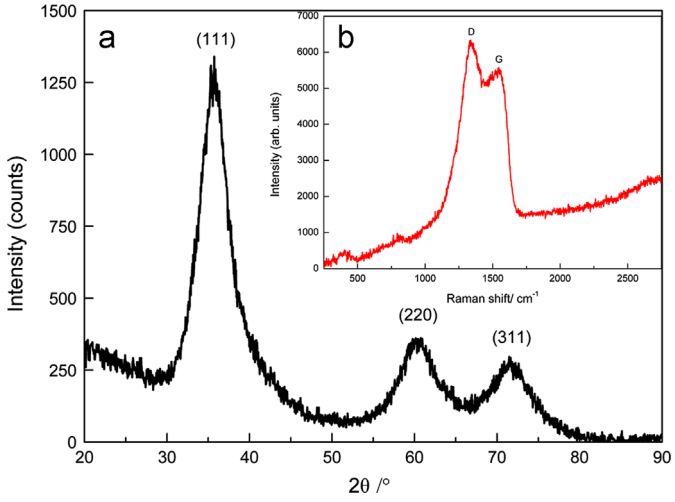


Fig. 4. (a) XRD pattern and (b) Raman spectrum of prepared SiC interphase.

### 3.2.2. *Effects of oxidation temperature on mechanical properties*

Anti-oxidation capability of composites with BN/SiC dual-layer interphase is also studied. Fig. 8 displays the stress–displacement curves of $SiC_f$/SiC composites with interphase oxidized at 800, 900 and 1000 °C for 6 h. It is revealed that the composites still exhibit standard toughened fracture behavior and the flexural strength decreases gradually from 208 to

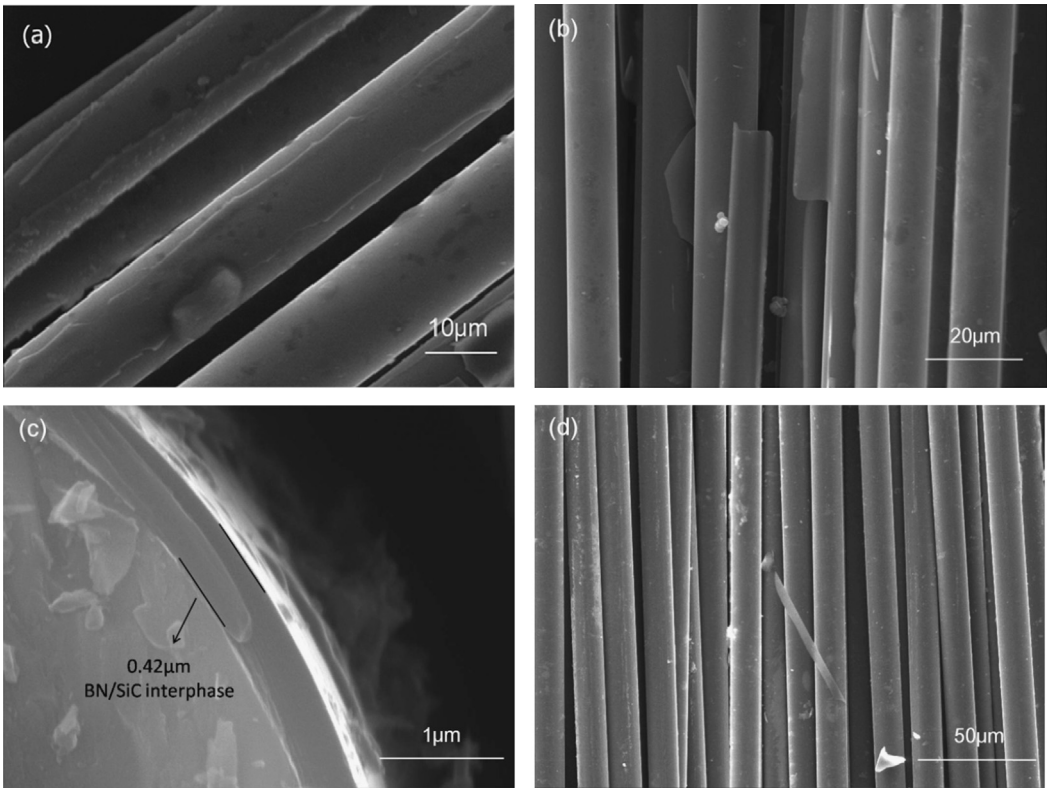


Fig. 5. Surface morphologies of the SiC fibers with BN/SiC dual-layer interphase.

Table 1
Properties of the fabricated $SiC_f$/SiC composites.

| Sample | Density (g $cm^{-3}$) | Porosity (%) | Flexural strength (MPa) | Failure displacement (mm) |
|---|---|---|---|---|
| (a) | 2.28 | 12.2 | 126(6[a]) | $0.14 \pm 0.01$ |
| (b) | 2.19 | 13.4 | 272(11) | $0.26 \pm 0.01$ |

[a]Numbers in parentheses represent standard deviations for flexural strength.

152 MPa with oxidation temperatures increasing from 800 to 1000 °C.

Fig. 9 shows comparison of flexural strength retentions of $SiC_f$/SiC composites with BN interphase and BN/SiC dual-layer interphase oxidized at 800, 900 and 1000 °C for 6 h. It is revealed that the flexural strength retention of composites with dual-layer interphase is much higher than that of composites with BN interphase over the whole oxidation temperature range. In the process of thermal oxidation, the microcracks and pores existing in the composites can be channels for oxygen to diffuse into the interior of the composites. As oxidation temperature increases, the matrix and SiC sub-layer would react with the diffused oxygen and silica forms on the surface of SiC materials. Eventually, the glassy silica can efficiently prevent further diffusion of oxygen and insulate the SiC fibers with oxygen. In addition, the BN sub-layer can arrest residual oxygen also, which will inhibit degradation of mechanical properties of the composites.

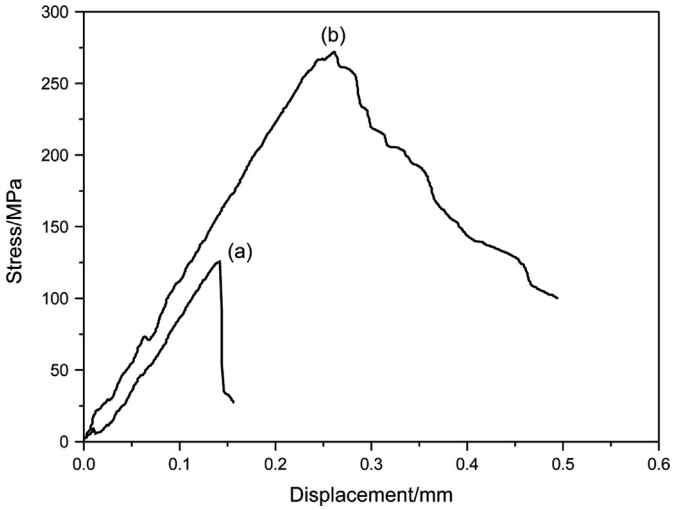


Fig. 6. Stress–displacement curves of $SiC_f$/SiC composites: (a) without interphase and (b) with BN/SiC dual-layer interphase.

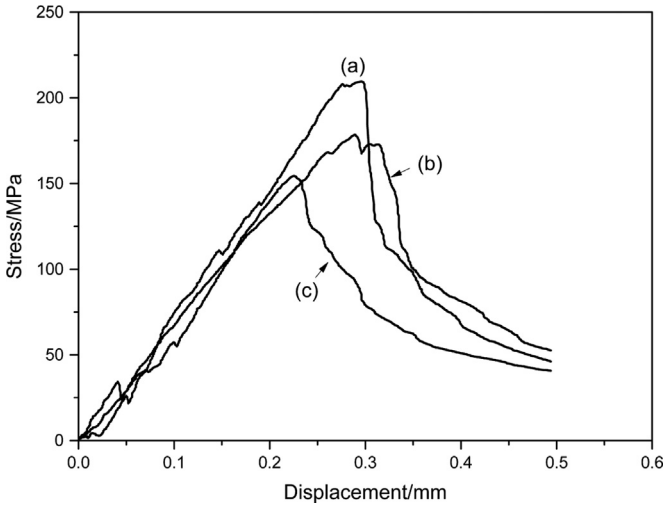


Fig. 8. Stress–displacement curves of $SiC_f$/SiC composites with BN/SiC dual-layer interphase oxidized at different temperatures for 6 h: (a) 800 °C, (b) 900 °C and (c) 1000 °C.

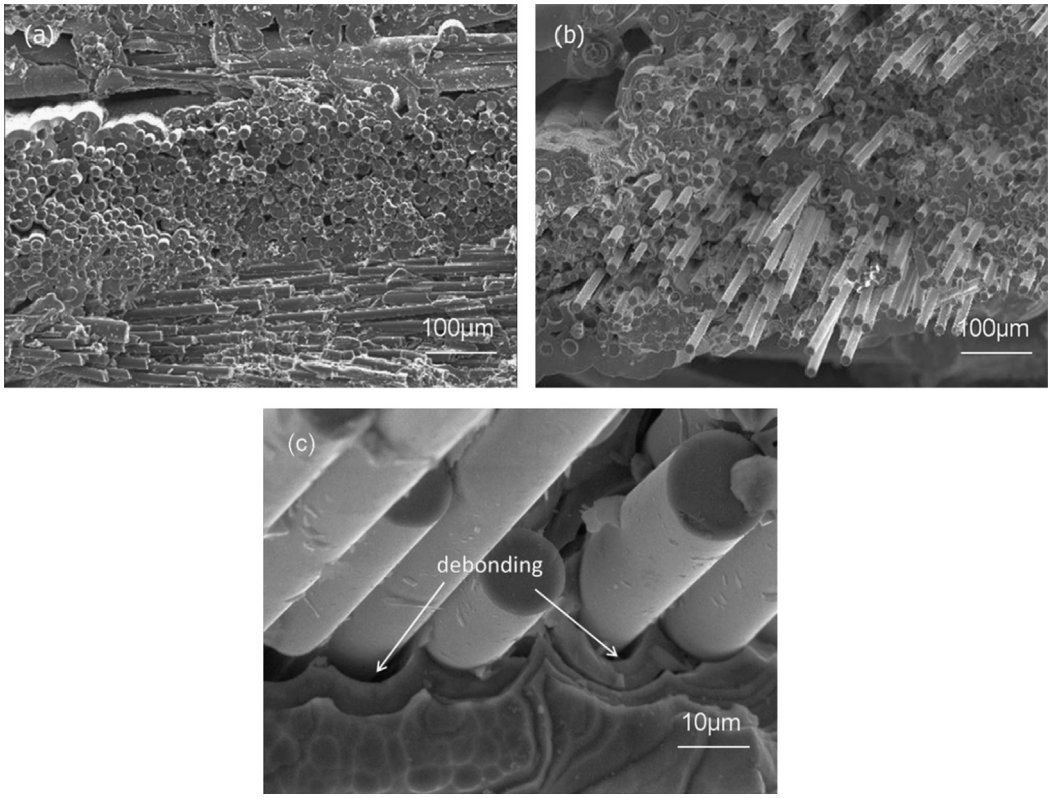


Fig. 7. Fracture surface morphologies of $SiC_f$/SiC composites: (a) without interphase and (b, c) with BN/SiC dual-layer interphase.

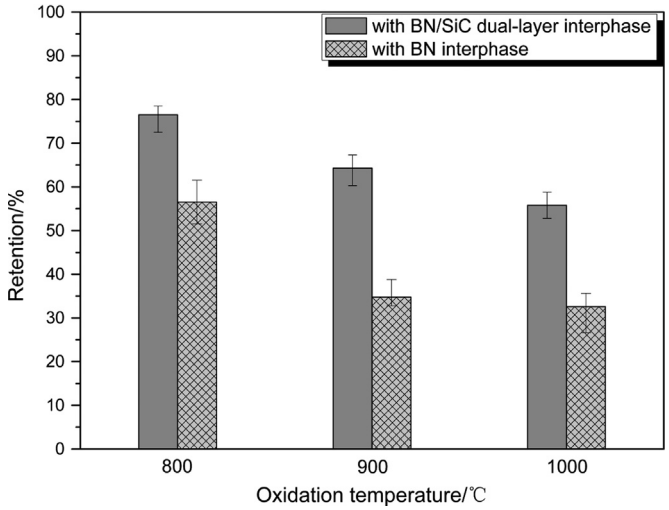


Fig. 9. Comparison of flexural strength retentions of $SiC_f$/SiC composites with BN interphase and BN/SiC dual-layer interphase oxidized at different temperatures for 6 h.

### 3.3. Dielectric properties of $SiC_f$/SiC composites with BN/SiC dual-layer interphase

Fig. 10 displays comparison of complex permittivity for $SiC_f$/SiC composites without interphase, with BN interphase and with BN/SiC dual-layer interphase. For composites without interphase, $\varepsilon'$ and $\varepsilon''$ of complex permittivity have the values of 30 and 22 respectively and are constant basically within the measured frequency range. It is revealed that the complex permittivity of composites with BN interphase is consistent with that of composites without interphase, indicating that BN has little influence on the dielectric properties of $SiC_f$/SiC composites. However, after BN/SiC interphase preparation, $\varepsilon'$ and $\varepsilon''$ of the composites increase remarkably to 45 and 32 respectively.

In the SiC materials, possible mechanisms for the polarization are electronic polarization, space charge polarization, relaxation polarization and reorientation polarization. The increase of $\varepsilon'$ could be attributed to relaxation polarization enhanced by more dangling bonds and vacancies [31,32]. And the larger $\varepsilon''$, suggesting better capacity of dielectric loss in the microwave frequency range, is usually associated with increased electrical conductivity. For the SiC matrix deposited from MTS, it has been confirmed that the CVD-SiC mainly consists of excess carbon and β-SiC crystals including many silicon and carbon lattice defects [33,34]. Under an alternating electromagnetic field, the reorientation of these lattice defects pairs results in polarization and energy dissipation, contributing to an increase of $\varepsilon'$. Owing to the existence of excess carbon in the matrix and PyC surface layer on the SiC fibers, $\varepsilon''$ is also remarkably enhanced, induced by the conductance losses. As a result, the as-received $SiC_f$/SiC composites exhibit a relatively high complex permittivity.

Compared to the composites without interphase, it can be concluded that the improvement of complex permittivity for the composites with dual-layer interphase is mainly ascribed to the PIP-SiC layer. The SiC pyrolysis from PCS is a complicated process, so highly pure SiC is difficult to be obtained. As discussed above, it can be confirmed that the PIP-SiC is incompletely crystalline and has carbon excess. The excess carbon in the SiC sub-layer is in the form of nano-crystals graphite dispersed around SiC crystals or in amorphous Si–C–O phase, which can form relatively continuous conductive network and play an important role in its electric properties [35]. Thus, it can be confirmed that all the components, including fibers, matrix and interphase, contribute to the enhancement of complex permittivity for the composites with interphase.

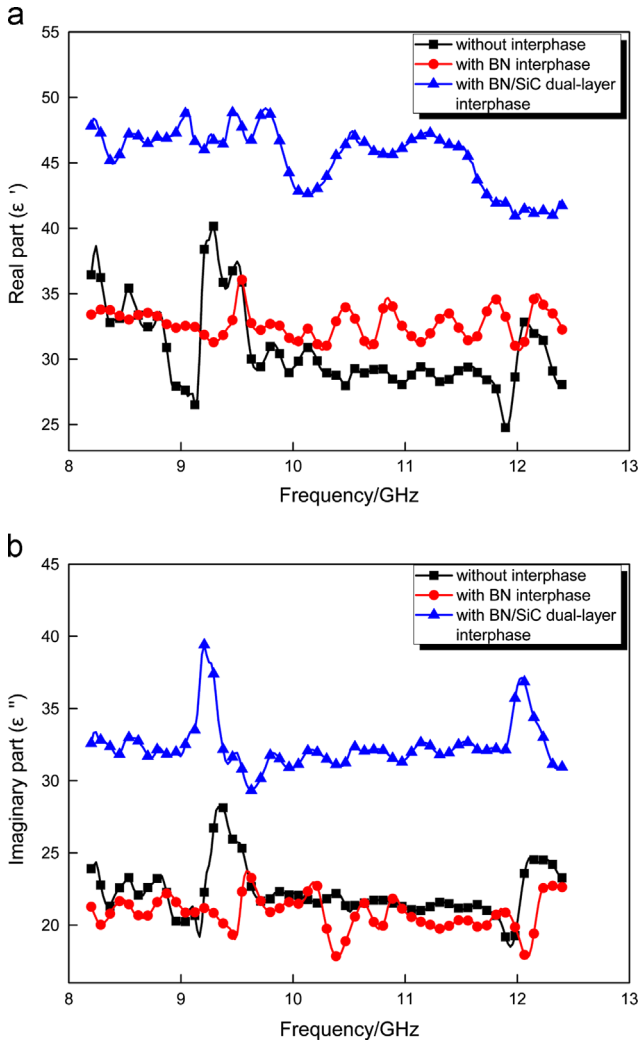


Fig. 10. (a) Real part and (b) imaginary part of complex permittivity as a function of frequency in the range of 8.2–12.4 GHz for $SiC_f$/SiC composites without interphase, with BN interphase and with BN/SiC dual-layer interphase.

## 4. Conclusions

BN/SiC dual-layer interphase in $SiC_f$/SiC composites was successfully prepared and its microstructure and surface morphology were characterized by XRD, Raman spectrum and SEM. The results show that the BN sub-layer processed by dip-coating and SiC sub-layer by PIP both have relatively low crystalline degree, and the SiC layer is carbon excess. Smooth and homogeneous surface morphology of the dual-layer interphase can be observed

from SEM images and its thickness is 0.42 μm. Mechanical measurements results show that the flexural strength and failure displacement of $SiC_f$/SiC composites are improved conspicuously from 126 MPa and 0.14 mm, respectively, to 272 MPa and 0.26 mm after preparation of BN/SiC dual-layer interphase. The flexural strength retention of composites with dual-layer interphase is much higher than that of composites with BN interphase over the oxidation temperature range from 800 to 1000 °C. The complex permittivity of the composites increases remarkably from $30-i22$ to $45-i32$ with the incorporation of dual-layer interphase, whose real and imaginary parts are associated with relaxation polarization and conductance losses established in the components, including fibers, matrix and interphase.

## Acknowledgments

This work was supported by Chinese National Natural Science Foundation (Grant no. 51072165) and the Fund of the State Key Laboratory of Solidification Processing in Northwestern Polytechnical University (No. KP201307).

## References

[1] R. Naslain, SiC–matrix composites: nonbrittle ceramics for thermostructural application, International Journal of Applied Ceramic Technology 2 (2005) 75–84.
[2] R. Naslain, Design, preparation and properties of non-oxide CMCs for application in engines and nuclear reactors: an overview, Composites Science and Technology 64 (2004) 155–170.
[3] H.J. Yu, X.G. Zhou, W. Zhang, Mechanical properties of 3D KD-I SiCf/SiC composites with engineered fibre–matrix interfaces, Composites Science and Technology 71 (2011) 699–704.
[4] H.T. Liu, H.F. Cheng, J. Wang, Microstructural investigations of the pyrocarbon interphase in SiC fiber-reinforced SiC matrix composites, Materials Letters 63 (2009) 2029–2031.
[5] K. Shimoda, T. Hinoki, A. Kohyama, Influence of pyrolytic carbon interface thickness on microstructure and mechanical properties of SiC/SiC composites by NITE process, Composites Science and Technology 68 (2008) 98–105.
[6] J.S. Li, C.R. Zhang, B. Li, Preparation and characterization of boron nitride coatings on carbon fibers from borazine by chemical vapor deposition, Applied Surface Science 257 (2011) 7752–7757.
[7] H.T. Wu, M.W. Chen, X. Wei, Deposition of BN interphase coatings from B-trichloroborazine and its effects on the mechanical properties of SiC/SiC composites, Applied Surface Science 257 (2010) 1276–1281.
[8] Y. Mu, W.C. Zhou, D.H. Ding, Influence of dip-coated boron nitride interphase on mechanical and dielectric properties of $SiC_f$/SiC composites, Materials Science and Engineering A 578 (2013) 72–79.
[9] H.J. Yu, X.G. Zhou, W. Zhang, Mechanical behavior of $SiC_f$/SiC composites with alternating PyC/SiC multilayer interphases, Materials & Design 44 (2013) 320–324.
[10] T. Taguchi, T. Nozawa, N. Igawa, Fabrication of advanced SiC fiber/F-CVI SiC matrix composites with SiC/C multi-layer interphase, Journal of Nuclear Materials 329–333 (2004) 572–576.
[11] E.Y. Sun, R. Nutt, J. Brennan, Fiber coatings for SiC-fiber-reinforced BMAS glass-ceramic composites, Journal of the American Ceramic Society 80 (1997) 261–266.
[12] R.T. Bhatt, Y.L. Chen, G.N. Morscher, Microstructure and tensile properties of BN/SiC coated Hi-Nicalon, and Sylramic SiC fiber preforms, Journal of Materials Science 37 (2002) 3991–3998.
[13] R.J. Kerams, R.S. Hay, T.A. Parthasarathy, M.K. Clinibulk, Interface design for oxidation-resistant ceramic composites, Journal of the American Ceramic Society 85 (2002) 2599–2632.
[14] F. Rebillat, J. Lamon, R. Naslain, Properties of multilayerd interphases in SiC/SiC chemical-vapor-infiltrated composites with "weak" and "strong" interfaces, Journal of the American Ceramic Society 81 (1998) 2315–2326.
[15] D.H. Ding, W.C. Zhou, F. Luo, Influence of pyrolytic carbon coatings on complex permittivity and microwave absorbing properties of $Al_2O_3$ fiber woven fabrics, Transactions on Nonferrous Metals Society of China 22 (2012) 354–359.
[16] H.T. Liu, H. Tian, Mechanical and microwave dielectric properties of $SiC_f$/SiC composites with BN interphase prepared by dip-coating process, Journal of the European Ceramic Society 32 (2012) 2505–2512.
[17] H. Tian, H.T. Liu, H.F. Cheng, Effects of SiC contents on the dielectric properties of $SiO_{2f}/SiO_2$ composites fabricated through a sol–gel process, Powder Technology 239 (2013) 374–380.
[18] H.T. Liu, H. Tian, H.F. Cheng, Dielectric properties of SiC fiber-reinforced SiC matrix composites in the temperature range from 25 to 700 °C at frequencies between 8.2 and 18 GHz, Journal of Nuclear Materials 432 (2013) 57–60.
[19] Q. Li, X.W. Yin, W.Y. Duan, Electrical, dielectric and microwave-absorption properties of polymer derived SiC ceramics in X band, Journal of Alloys and Compounds 565 (2013) 66–72.
[20] D.F. Lii, J.L. Huang, L.J. Tsui, Formation of BN films on carbon fibers by dip-coating, Surface and Coatings Technology 150 (2002) 269–276.
[21] S. Le Gallet, G. Chollon, F. Rebillat, A. Guette, Microstructural and microtextural investigations of boron nitride deposited from $BCl_3$–$NH_3$–$H_2$ gas mixtures, Journal of the European Ceramic Society 24 (2004) 33–44.
[22] D.H. Ding, W.C. Zhou, F. Luo, Mechanical properties and oxidation resistance of $SiC_f$/CVI-SiC composites with PIP-SiC interphase, Ceramics International 38 (2012) 3929–3934.
[23] H.T. Liu, H.F. Cheng, J. Wang, Effects of the single layer CVD SiC interphases on the mechanical properties of the $SiC_f$/SiC composites fabricated by PIP process, Ceramics International 36 (2010) 2033–2037.
[24] J.S. Ha, K.K. Chawla, Effect of SiC/BN double coating on fibre pullout in mullite fibre/mullite matrix composites, Journal of Materials Science Letters 12 (1993) 84–86.
[25] Y. Cheng, X.W. Yin, Y.S. Liu, BN coatings prepared by low pressure chemical vapor deposition using boron trichloride–ammonia–hydrogen–argon mixture gases, Surface and Coatings Technology 204 (2010) 2797–2802.
[26] P. Colombo, G. Mera, R. Riedel, G.D. Soraru, Polymer-derived ceramics: 40 years of research and innovation in advanced ceramics, Journal of the American Ceramic Society 93 (2010) 1805–1837.
[27] Y. Ma, S. Wang, Z.H. Chen, Raman spectroscopy studies of the high-temperature evolution of the free carbon phase in polycarbosilane derived SiC ceramics, Ceramics International 36 (2010) 2455–2459.
[28] W. Yang, A. Kohyama, T. Noda, Interfacial characterization of CVI-SiC/SiC composites, Journal of Nuclear Materials 307–311 (2002) 1088–1092.
[29] R. Naslain, The design of the fibre-matrix interfacial zone in ceramic matrix composites, Composites Part A: Applied Science and Manufacturing 29 (1998) 1145–1155.
[30] H.T. Liu, H.F. Cheng, J. Wang, Effects of the fiber surface characteristics on the interfacial microstructure and mechanical properties of the KD SiC fiber reinforced SiC matrix composites, Materials Science and Engineering A 525 (2009) 121–127.
[31] X.M. Li, L.T. Zhang, X.W. Yin, Mechanical and dielectric properties of porous $Si_3N_4$–SiC (BN) ceramic, Journal of Alloys and Compounds 490 (2010) L40–L43.
[32] G.P. Zheng, X.W. Yin, J. Wang, Complex permittivity and microwave absorbing property of $Si_3N_4$–SiC composite ceramic, Journal of Materials Science & Technology 28 (2012) 745–750.
[33] H.T. Liu, H.F. Cheng, J. Wang, Dielectric properties of the SiC fiber-reinforced SiC matrix composites with the CVD SiC interphases, Journal of Alloys and Compounds 491 (2010) 248–251.
[34] X.M. Yu, W.C. Zhou, F. Luo, Effect of fabrication atmosphere on dielectric properties of SiC/SiC composites, Journal of Alloys and Compounds 479 (2009) L1–L3.
[35] D.H. Ding, W.C. Zhou, B. Zhang, Complex permittivity and microwave absorbing properties of SiC fiber woven fabrics, Journal of Materials Science 46 (2011) 2709–2714.